

DOCUMENTS

D GVTDOC
D 211.
9:
3809

ad 745 729

NAVAL SHIP RESEARCH AND DEVELOPMENT CENTER

Bethesda, Md. 20034



MONITORING STRESS WAVE EMISSIONS

by

Hendrikus H. Vanderveldt

APPROVED FOR PUBLIC RELEASE: DISTRIBUTION UNLIMITED

STRUCTURES DEPARTMENT
RESEARCH AND DEVELOPMENT REPORT

20070122018

June 1972

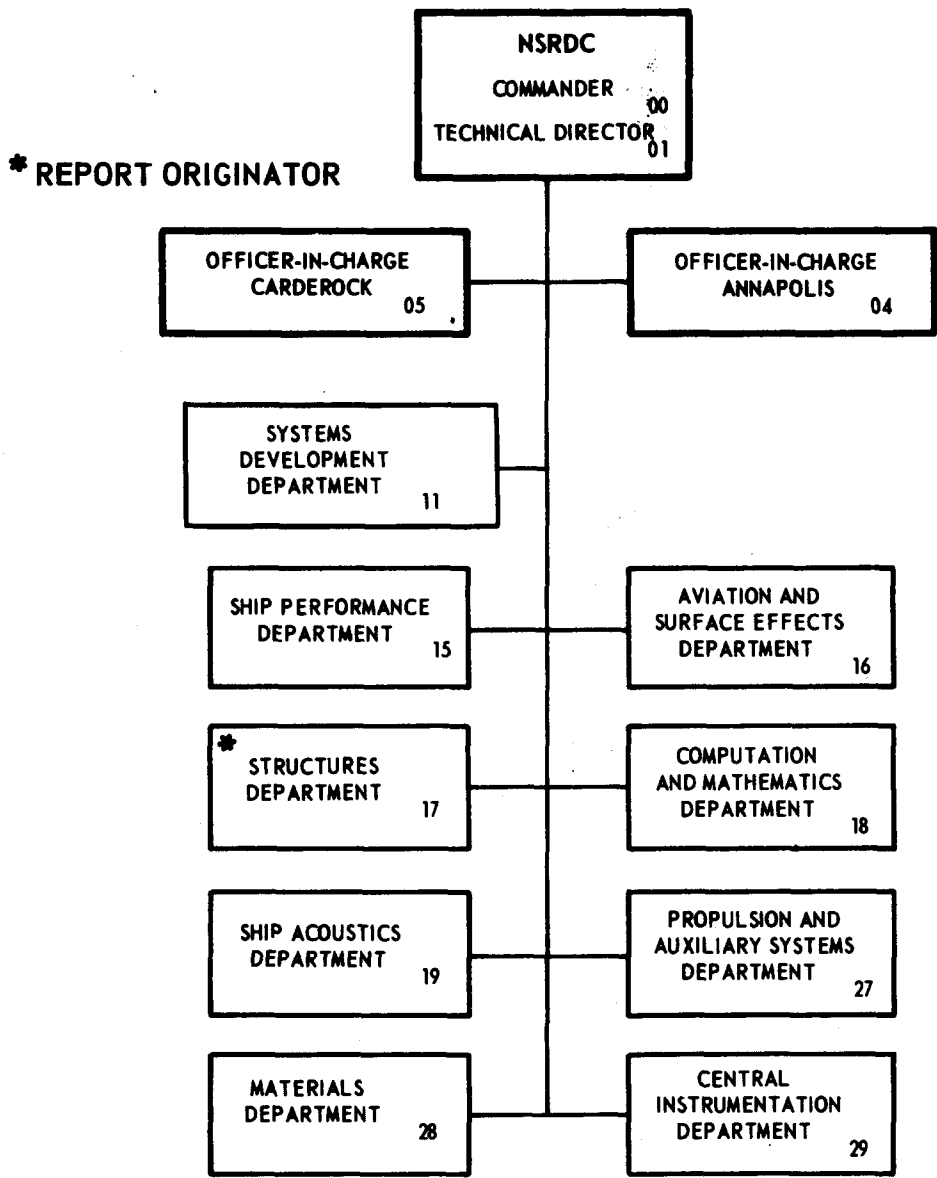
REPORT 0000

MONITORING STRESS WAVE EMISSIONS

The Naval Ship Research and Development Center is a U. S. Navy center for laboratory effort directed at achieving improved sea and air vehicles. It was formed in March 1967 by merging the David Taylor Model Basin at Carderock, Maryland with the Marine Engineering Laboratory at Annapolis, Maryland.

Naval Ship Research and Development Center
Bethesda, Md. 20034

MAJOR NSRDC ORGANIZATIONAL COMPONENTS



DEPARTMENT OF THE NAVY
NAVAL SHIP RESEARCH AND DEVELOPMENT CENTER
BETHESDA, MD. 20034

MONITORING STRESS WAVE EMISSIONS

by
Hendrikus H. Vanderveldt



APPROVED FOR PUBLIC RELEASE: DISTRIBUTION UNLIMITED

June 1972

Report 3809

TABLE OF CONTENTS

	Page
ABSTRACT	1
ADMINISTRATIVE INFORMATION	1
BACKGROUND	1
APPLICATIONS TO DATE	4
WELD MONITORING	4
SUBCRITICAL CRACK GROWTH	5
STRESS CORROSION CRACKING	8
MATERIAL STUDIES	11
SYSTEM DESIGN	13
ACOUSTIC EMISSION, SOURCES AND DETECTION METHODS	16
SIGNAL CONDITIONER	18
DATA ANALYSIS	22
SYSTEM CONSTRUCTION	27
SYSTEM APPLICATION	29
FUTURE PLANS	32
SUMMARY	34
ACKNOWLEDGMENTS	35
REFERENCES	35

LIST OF FIGURES

Figure 1 - Artist's Concept of Potential Application of System for Monitoring Stress Wave Emissions	3
Figure 2 - Experimental and Theoretical Results of dN/dn versus Number of Fatigue Cycles	7
Figure 3 - Comparison of Actual and Predicted Crack-Growth Rates for Hydrogenated D6aC Steel	10
Figure 4 - Prediction of Observed Crack-Jump Distance, Based upon Approximate Dislocation Mobility Model	14
Figure 5 - Schematic of System for Monitoring Stress Wave Emissions	15
Figure 6 - Frequency Range of Various Emission Sources	17
Figure 7 - Frequency Range of Various Types of Transducers	17

	Page
Figure 8 - Schematic of Signal Conditioner	19
Figure 9 - Level Detector	21
Figure 10 - Digital Filter	21
Figure 11 - Slope Detector	23
Figure 12 - Interface	23
Figure 13 - Schematic of Recycle Timer	25
Figure 14 - System for Monitoring Stress Wave Emissions	28
Figure 15 - Two Glass Hemispheres Subjected to Compressive Loadings	30
Figure 16 - Transducer Layout on Glass Hemispheres	31
Figure 17 - Level Recording from Glass Hemispheres	33

ABSTRACT

Basic principles of the acoustic-emission technique used at the Center are discussed, and a review of some applications of the method are presented. Potential capabilities and drawbacks to naval applications are summarized; finally, a description of the design and construction of the present monitoring capability at the Naval Ship Research and Development Center is presented.

ADMINISTRATIVE INFORMATION

The work described in this report was authorized and funded primarily by the Deep-Submergence Systems Project under Task Area S4616, Task 11896. The original design of the acoustic-emission system, since extensively modified, was developed by Aerojet General Corporation under contract to the Naval Ship Research and Development Center and was funded under Naval Ship Systems Command (NAVSHIPS) Task Area S-F35.422.303, Task 2047. In fiscal years 1971 and 1972, sponsorship of the acoustic-emission effort was under NAVSHIPS Task Area S-F51.541.009, Task 15961, and Task Area S-F51.541.003, Task 15961.

BACKGROUND

A material or structure that undergoes deformations or microcracking sends out small quantities of energy. With the use of proper transducers these "energy pulses" may be detected. This phenomenon was first reported by Kaiser¹ in 1950. The terms "acoustic emission" or "stress wave emission" have been applied to describe these energy pulses. The precise nature of acoustic emission is still not well understood, although various researchers have suggested that the emissions are due to plastic deformation, such as grain boundary slippage and dislocation movement, or to micro- or macro-cracking.

¹Kaiser, J., "Untersuchungen uber das auftreten Gerauschen beim Zugversuch," Ph.D. thesis, Technische Hochschule, Munich (1950). A complete listing of references is given on page 35.

One of the primary reasons that the acoustic emissions are of interest to the Navy is that emission sources can be located using triangulation techniques. These triangulation techniques utilize the difference in time of arrival of the pulses to at least three transducers spaced some known distances apart. Knowledge of the speed at which the pulse travels together with the time of arrival differences at three transducers enable location of the source of the emission. With the advent of structures that utilize new materials with high strength but limited toughness, the presence of flaws becomes increasingly significant. Consequently determining not only the presence but also the location of flaws is critical to the investigator so that further nondestructive evaluation (NDE) methods may be applied to determine the severity of the flaws. (Figure 1 is a cartoon illustrating some of the failure modes considered on present naval structures.)

In naval applications, other potential advantages of a monitoring system for stress wave emissions may include:

1. A definitive certification record that will exist for each structure.
2. Considerable reduction of the need for frequent structural inspection of the fleet gained from a thorough knowledge of the existence of flaws and acoustic-emission sources in a structure.
3. Significant increase in the reliability of the structures in the fleet.
4. Extension of the service life of the structure without loss in the reliability, since the flaws in the structure will be well known.
5. Location of other deficiencies that are acoustically detectable within naval structures.
6. Improved and/or increased data obtainable from standard tests in laboratory applications.
7. A significant advance in the array of nondestructive testing (NDT) equipment available to the Navy.

Developing a monitoring system for stress wave emissions, however, does have some inherent difficulties. These include:

1. Present ability of the system to locate only dynamic events, i.e., growing plastic zone or growing cracks.

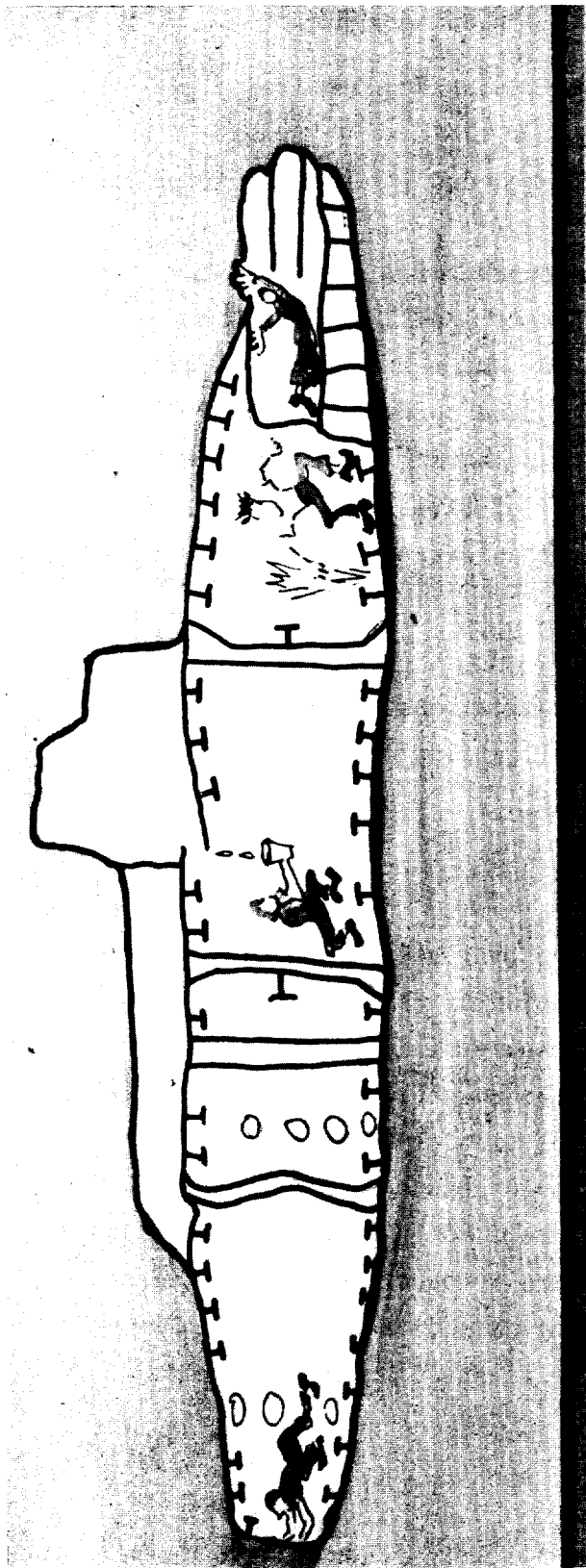


Figure 1 - Artist's Concept of Potential Application of System for Monitoring Stress Wave Emissions

2. Present state-of-the-art requirement for a material characterization for each material being monitored.

3. Formidable obstruction caused by background noise, e.g. cavitation.

4. Dependence on dynamic events precludes replacement of other NDT methods.

5. High cost of the initial development of a usable system.

At the present time the long range advantages appear to have the upper hand. It is emphasized that although other NDT methods are not replaced, the stress wave emission monitoring can locate potentially critical flaws in inaccessible locations. Additionally monitoring stress wave emissions is economically sound, if the service life of naval vehicles can be extended and the number of structural overhauls can be reduced.

APPLICATIONS TO DATE

In the last few years, numerous applications of monitoring stress wave emissions have been made. A few applications of special interest to the Navy will be discussed.

WELD MONITORING

Welds in structural components have long been known to experience cracking from shrinkage long after completion of the actual welding operation. In critical structures such as pressure vessels, the designer has frequently specified a waiting period after completion of the last welding pass for as much as 1 week to ensure completion of the delayed weld cracking. Monitoring stress wave emissions could reduce such waiting periods significantly by listening to the structure. Monitoring acoustic emissions has shown that delayed weld cracking generally occurs within the first 30 hr after completion of the last welding pass on a structure. The major portion of the activity occurs within the first 10 hr after completion of the last welding pass.

Specifically, Jolly² reported about acoustic emissions during and immediately after completion of the welding. Jolly found that acoustic emission occurred from 20 to 40 sec after a defect region began to solidify. Additionally a direct correlation was obtained between radiographic analysis of welds and the acoustic emission for 1/8- and 1/2-in.-thick 304L stainless steel as well as for 1/2-in.-thick 316 stainless steel plate.

In a study concerned with monitoring the stress wave emission in HY-80 steel, Hartbower³ reported acoustic emissions as long as 55 hr after completion of the welding. The test specimen was HY-80 steel in the form of plate sections 0.70 × 2 × 10 in., welded together to form a 0.70 × 8 × 10-in. plate. A significant point to make is that such monitoring of stress wave emissions can be done without the need to have operators present.

SUBCRITICAL CRACK GROWTH

The integrity of structures can be deleteriously affected by subcritical crack growth. Many mechanisms may cause such crack growth. Of particular interest to the Navy are fatigue and corrosion. Monitoring stress wave emissions is playing a useful role in defining detailed mechanisms in fatigue and corrosion as will be discussed in the following paragraphs.

A recent contribution by Dunegan et al.⁴ addressed monitoring stress wave emissions to the problem of fatigue. The basic fatigue

²Jolly, W. D., "Acoustic Emission Exposes Cracks during Welding," Welding Journal Vol. 48, No. 1, pp. 21-27 (Jan 1969).

³Hartbower, C. E., "Application of Stress Wave Analysis Technique to the Nondestructive Inspection of Welds, Welding Journal, Vol. 49, No. 2, p. 54S (Feb 1970).

⁴Dunegan, H. L. et al., "Detection of Fatigue Crack Growth by Acoustic Emission Techniques," Materials Evaluation Journal, Vol. 28, No. 10, pp. 221-227 (Oct 1970).

crack growth equation proposed by Paris⁵ was used in the discussion, i.e.,

$$\frac{da}{dn} = C K^q \quad (1)$$

where a is the crack length,

n is the number of cycles,

C is a constant,

K is the range of the applied stress intensity, and

q is an empirically determined exponent.

A relationship between the total number of acoustic emissions N and the stress intensity was shown to be feasible by Dunegan et al. It is given by

$$N = A K^m \quad (2)$$

where A is a constant, and m is an empirically determined exponent.

Equations (1) and (2) can be combined to relate the number of emissions per fatigue cycle to the crack-growth rate during that cycle. However acoustic emissions are irreversible; thus, after the first cycle, emissions will cease unless K changes.

To make monitoring acoustic emissions feasible in fatigue of a structural element Dunegan et al. suggested periodic proof-testing at a higher K than the fatigue K. Thereby acoustic emissions would be obtained only if K had increased between proof-tests. It was found in Reference 4 that for a trip-steel wedge opening-loaded (WOL) specimen, the count rate increased rapidly as failure approached. Since the actual count is relative, the count over a number of fatigue cycles was found, i.e., dN/dn. Results are shown in Figure 2. The theoretical predictions are conservative and are made using known relations given in Equations (1) and (2) for trip steel.

⁵Paris, P. C., "The Fracture Mechanics Approach to Fatigue," Proceedings 10th Sagamore Conference, Syracuse University Press, N. Y., p. 107 (1965).

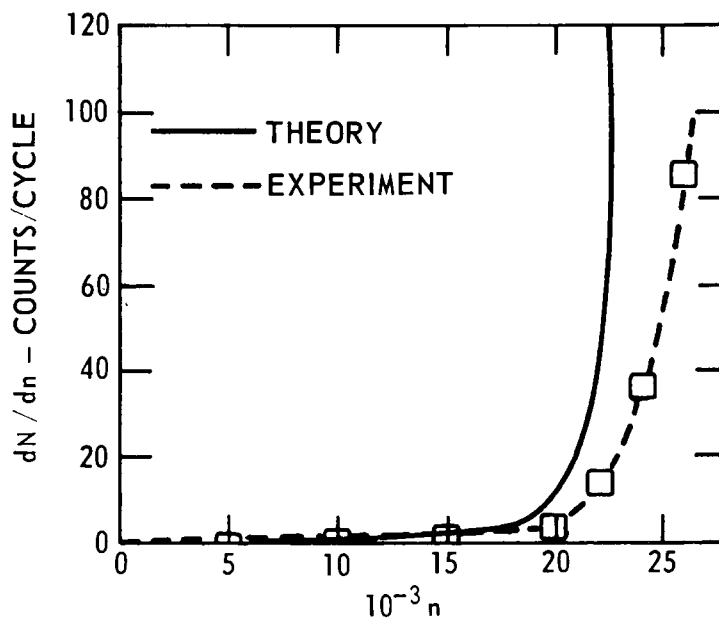


Figure 2 - Experimental and Theoretical Results of dN/dn versus Number of Fatigue Cycles

Finally, Dunegan et al. noted that acoustic emissions, while holding at the proof load, increased as the number of cycles increased. The authors commented as follows that noticeable continuing emissions only occurred at holding-stress intensities greater than $63 \text{ ksi}\sqrt{\text{in}}$.

"This is important information from a nondestructive testing viewpoint, because if emission was not observed under constant load, the stress intensity factor for any flaw that may be present is less than $63 \text{ ksi}\sqrt{\text{in}}$."

The area of acoustic emissions in fatigue analysis still requires extensive investigation; however, at this time it appears to be feasible.

STRESS CORROSION CRACKING

Acoustic emission has been used to study stress corrosion cracking. The discussion that follows is based on Reference 6. The crack growth that occurs under conditions of stress corrosion cracking can be monitored through the presence of stress wave emissions. Therefore the use of acoustic emission to accurately establish incubation time in stress corrosion cracking such as for hydrogen induced cracking becomes apparent. Gerberich and Hartbower⁷ have reported some results using this technique and a few aspects of their investigation will be discussed here. The incubation time in question is the time required for a crack to reinitiate from an initially existing fatigue precrack with the causative agent being stress corrosion cracking. In other words the standard experimental fracture mechanics approach will be followed. During growth of the crack the emissions may be monitored conveniently using acoustic detection methods. This experimental data may then be used to establish or verify some theoretical approach. One such analytical approach will be shown in the following paragraphs, and, although some of the analysis is rather crude, it is certainly not an exercise in academic futility.

Specifically the discussion will concern itself with hydrogen embrittlement. Hydrogen induced cracking comes about due to the diffusion of the hydrogen atom into the lattice for a specific critical distance S^* ahead of the crack tip. When the hydrogen concentration C becomes critical C_{cr} , then the matrix will fail over the distance S^* when subjected to a load. Exactly at the new crack tip, the hydrogen concentration is assumed to be the initial value C_0 so that the diffusion process starts all over and repeats. It is assumed that the small crack advances S^* occur at con-

⁶Lomacký, O. and H. Vanderveldt, "Critical Review of Fracture and Fatigue Analysis," NSRDC Report 3655 (1971).

⁷Gerberich, W. W. and C. E. Hartbower, "Monitoring Crack Growth of Hydrogen Embrittlement and Stress Corrosion Cracking by Acoustic Emission," Proceedings of Conference on Fundamental Aspects of Stress Corrosion Cracking, Ohio State University, National Association of Corrosion Engineers, pp. 420-438 (1967).

stant time intervals Δt_s . If the diffusivity D of the hydrogen into the lattice is known, then the buildup in C is governed approximately by

$$\frac{C_{cr} - C_o}{C_o} \cdot S^{*2} \approx 4D \Delta t_s \quad (3)$$

Based on some experimental evidence, i.e., the average facet size observed in the electron microscope, a value for S^* has been obtained empirically and is given by

$$S^* \approx \frac{C_{cr}}{C_o} d \quad (4)$$

where d is the average facet size as observed in the electron fractographs. It should be noted that the diffusivity D can be reduced by an order of magnitude (or two) if hydrogen traps are present.⁸ One necessary condition for local crack growth can be obtained by assuming that such an order of magnitude reduction occurs. Then the incubation time to initiate a local failure over a distance S^* may be computed as

$$\Delta t_s \approx \frac{(C_{cr} - C_o) C_{cr}^2 d^2}{40 C_o^3 D} \quad (5)$$

In addition to Equation (5) a minimum stress level must be achieved. Such a minimum stress requirement is satisfied in terms of a critical crack-tip displacement. It was also experimentally observed that the cracks moved in jumps that were for all practical purposes equal to the theoretical crack-tip displacement. With this knowledge the crack growth rate dc/dt may be computed

$$\frac{dc}{dt} \approx \frac{l^*}{\Delta t_s} \quad (6)$$

⁸Coe, F. R. and J. Morebon, "Estimation of Diffusibility Coefficients for Hydrogen in Ferrous Materials," British Welding Journal, Vol. 43 (1967).

where λ^* is the approximate jump distance. An approximate expression for λ^* is obtained by substitution of the expression for the theoretical crack-tip displacement into the relation between λ^* and the crack-tip displacement. The result is

$$\lambda^* = \frac{K^2}{m \sigma_o E \pi \epsilon_f} \quad (7)$$

where K is the stress intensity at the crack tip $m \approx 1$ for plane stress and $m \approx 2$ for plane strain,

σ_o is the yield stress, and

ϵ_f is the fracture ductility.

Combining Equations (5) and (6) and (7) results in an approximate expression for the growth rate

$$\frac{dc}{dt} \approx \frac{40 K^2 C_o^3 D}{m \sigma_o E \pi \epsilon_f (C_{cr} - C_o) C_{cr}^2 d} \quad (8)$$

Equation (8) is important because it provides a theoretical picture of the stress corrosion process due to hydrogen embrittlement. Additionally the equation can be verified, using acoustic emissions. One such comparison has been shown in Figure 3, which was taken from Reference 7. This approach indicates another path which may be followed in an attempt to understand the phenomenon of stress corrosion cracking, even though some significant

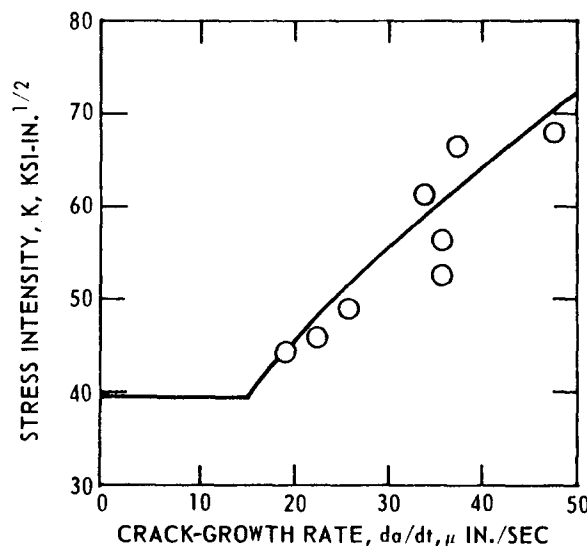


Figure 3 - Comparison of Actual and Predicted Crack-Growth Rates for Hydrogenated D6aC Steel

approximations have been used. It seems apparent also that without the use of acoustic emission-detection equipment, the problem of studying initiation times and growth per single crack is a formidable experimental problem.

MATERIAL STUDIES

Stress wave emissions have also been used to study fundamental phenomena other than stress-corrosion cracking. Data obtained using acoustic emissions have also been used to observe dislocation movement as well as crack growth. In the Ord study,⁹ acoustic-emission signals were directly related to dislocation movement, since considerable activity occurred in the initial part of the loading cycle.

In a recent study Frederick¹⁰ studied the dislocation mechanism as a source of acoustic emission. Frederick indicated that both the amount of the applied stress and the microstructure would affect the amount and level of acoustic emission. Specifically the effect of grain size was considered. It was found that the total acoustic emission count increased as the grain size ranged from very small to about 400 μ diameter; beyond that the total count rate dropped off again. It should be noted that this was for a special case. However an interesting trend had been observed.

In another fundamental study, Chambers¹¹ analyzed the spectrum from an acoustic emission during fatigue crack growth. Acoustic emissions were measured during the terminal phase of low-cycle, high-stress fatigue deformation in aluminum sheet samples. Acoustic emissions occurred primarily in the frequency band from 500 kHz to 1 MHz during the early stages of the fatigue failure test. As the fatigue crack progressed, Chambers found that the frequency band broadened and shifted downward. It would

⁹Ord, R. N., "Acoustic Emission Detection of Dislocation Movement and Crack Growth in HY-80 Ferritic Steel," Batelle Memorial Institute (NW) Report Y 49034 to the Naval Ship Research and Development Center (1969).

¹⁰Frederick, J. R., "Dislocation Mechanisms as Sources of Acoustic Emission," Presented at the Symposium on Advanced Nondestructive Testing Techniques, sponsored by Advanced Research Projects Agency and Army Materials and Mechanics Research Center, Watertown, Mass. (Jun 1971).

¹¹Chambers, R. H., "Time and Frequency Domain Analysis of Acoustic Emission during Fatigue Failure," Presented at the Symposium on Advanced Nondestructive Testing Techniques, sponsored by Advanced Research Projects Agency and Army Materials and Mechanics Research Center, Watertown, Mass. (Jun 1971).

seem from this result that spectral analysis can provide considerable information; however, these results are still in the exploratory stage and will need more work before such an analysis can be used on a practical basis.

Gerberich and Reuter¹² reported on applying stress wave emission to establish a theoretical model for predicting ductile fracture instability.* The small-amplitude continuous emissions were shown to be due to dislocation sources and could be fitted to the Gilman¹³ dislocation model, i.e.,

$$\rho_m = 10^5 m_p \epsilon_p e^{-\phi \epsilon_p} \quad (9)$$

where ρ_m is the mobile dislocation density,

m_p is a breeding factor,

ϵ_p is the plastic strain, and

$$\phi = H/\sigma_s,$$

where H is the hardening coefficient and σ_s is the root-mean-square shear stress.

Larger amplitude, but discontinuous stress wave emissions from a growing crack were used to establish the crack-jump distance. This distance was then equated to the region in front of the crack, where dislocation mobility reached a sufficiently low value to trigger fracture. The resulting theoretical equation is given by

$$\ell^* = \frac{\phi K^2}{3 \pi \sigma_{ys} E \ln (10^5 m_p)} \quad (10)$$

¹²Gerberich, W. W. and W. G. Reuter, "Theoretical Model of Ductile Fracture Instability Based on Stress-Wave Emission," Final Report to Office of Naval Research, Aerojet General Corporation Contract N00014-66-C-0340 (Feb 1969).

¹³Gilman, J. S., Proceedings of the Fifth U. S. National Congress on Applied Mechanics, American Society of Testing Materials, New York, p. 385 (1966)

*As will be recalled a similar approach was used to establish a model in the case of hydrogen embrittlement.

where l^* is the theoretical jump distance,
K is the applied stress intensity,
 σ_{ys} is the yield strength, and
E is the modulus of elasticity.

The experimentally determined jump distance showed good agreement with l^* as shown in Figure 4.

Other applications of the monitoring system for stress wave emissions have been made. The literature contains many of these. Consequently they will not be discussed in detail. Some of these applications include leak detecting, bridge monitoring, determining a proper level of prestress in prestressed concrete, and monitoring critical sections in cranes. The fundamental studies and practical engineering applications that can be monitored using these procedures are multiple and are limited only by the imagination of the investigator.

SYSTEM DESIGN

During the 1960's several electronic schemes were used in monitoring stress wave emissions. In this discussion various kinds of emission sources will be discussed and will be followed by a description of the detection, recording, signal processing, and analyzing systems. A schematic of the instrumentation planned for the Center system is shown in Figure 5. Basically, the transducer picks up the desired and undesired signals. Proper selection of a transducer will aid in later discriminatory steps. A preamplifier is located as physically close to the transducer as possible in order to improve the signal-to-noise ratio. Since the stress wave emission may be of very small amplitude, the effect of the noise picked by the line can be significant. The preamplifier in the line reduces that effect. These preamplifiers are commercially available.

From the preamplifier, the signal is sent through a broadband-pass filter to improve the fidelity of the signal, particularly since the signal will go through another preamplifier before any conditioning of the signal is done. Simply, the band-pass filter does the first clean-up on the signal.

From the band-pass filter, the signal can be recorded on tape for future analyses or can be channeled into the signal conditioner for

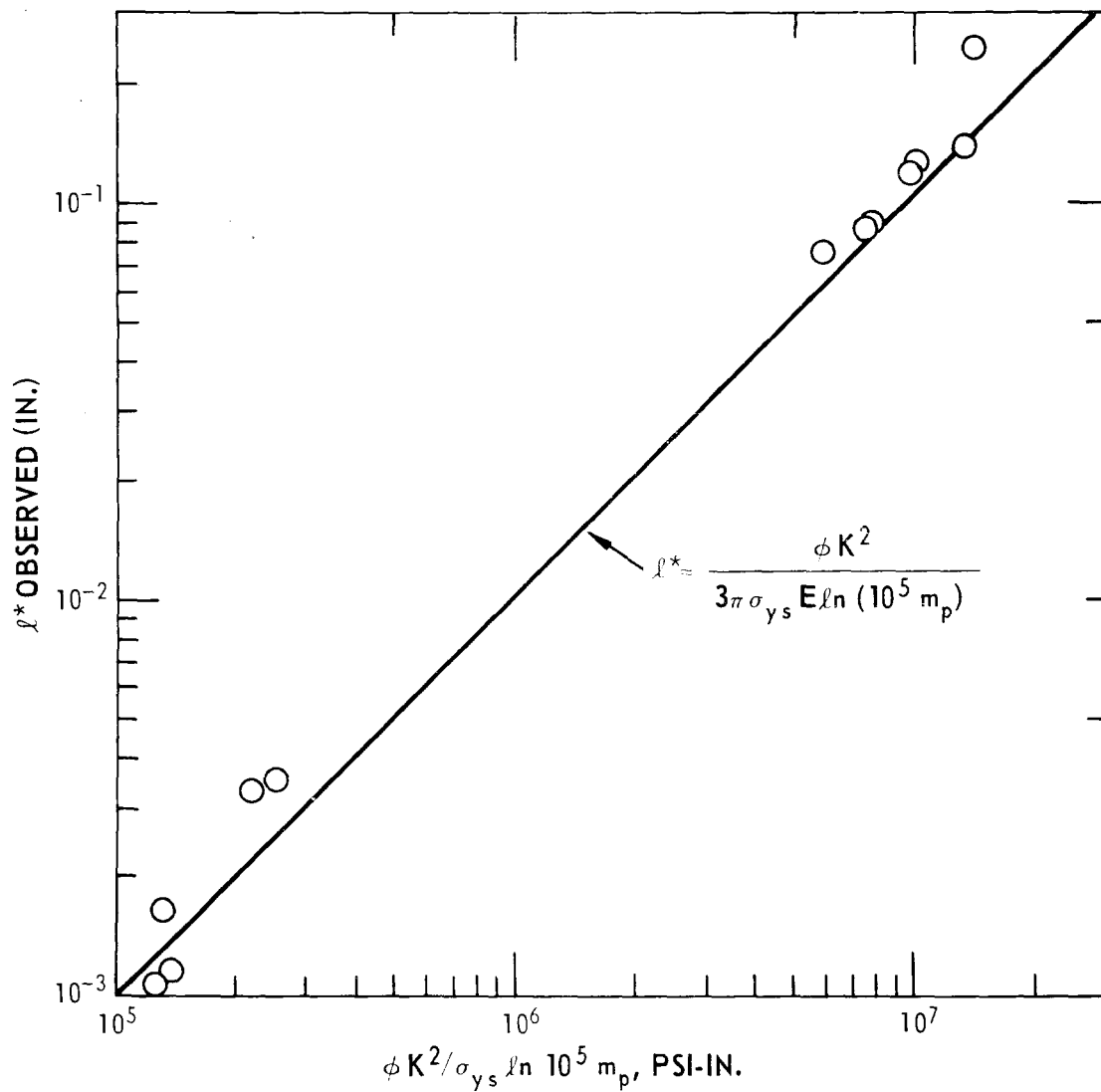


Figure 4 - Prediction of Observed Crack-Jump Distance, Based upon Approximate Dislocation Mobility Model

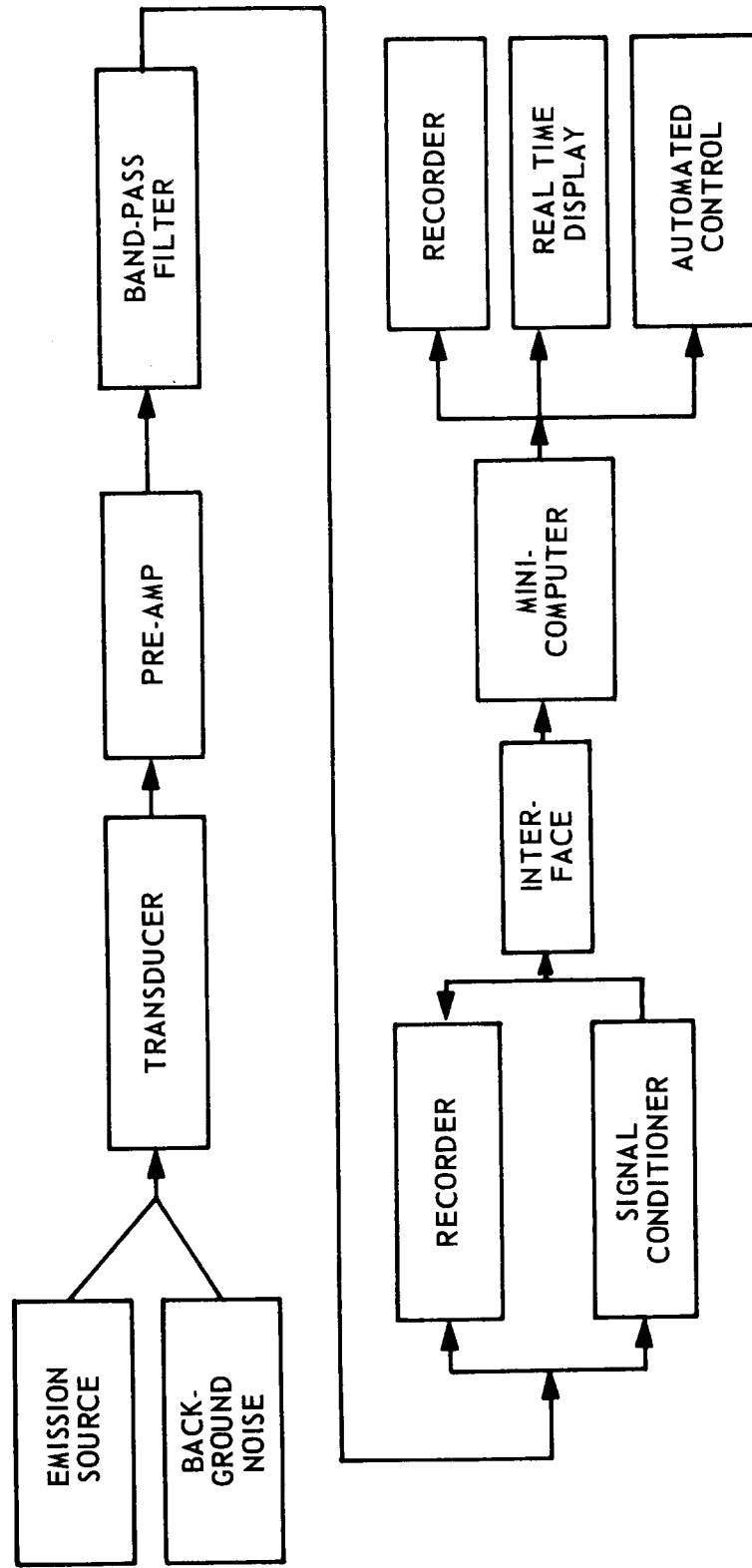


Figure 5 - Schematic of System for Monitoring Stress Wave Emissions

real-time analysis. In many cases the test may take a number of days. Then the recording system will consist of a continuous tape-loop recorder as well as a reel-to-reel recorder. The tape-loop recorder records all incoming data, and the reel-to-reel recorder stores only significant data. The real-time analysis is accomplished with the aid of a computer, which will be discussed in greater detail later.

ACOUSTIC EMISSION, SOURCES AND DETECTION METHODS

One of the primary difficulties encountered in analyzing acoustic emissions is the presence of extraneous signals. In Figure 6 the sound spectrum of frequently detectable signals has been shown. The range of the voice is unlikely to exceed 20 kHz (20,000 cycles per second). Commonly encountered, mechanically produced sound generally does not exceed 100 kHz. Hydraulic noise such as flow noise in piping is thought to be approximately 300 kHz, whereas cavitation noise probably has components that go higher than 700 kHz.¹⁴ Acoustic emissions, however, have been reported to occur at frequencies well into the megahertz (1000 kHz) range. Consequently the easiest method of discriminating acoustic emissions would appear to be in a band higher than the frequencies given by extraneous sources. A primary drawback however is the high attenuation of high-frequency shear* waves. Additionally the sensitivity of the sensor drops off at very high frequencies.

In Figure 7 the upper natural frequencies of various types of transducers have been shown. Microphones generally do not extend much more than 100 kHz, although some capacitance microphones are known to have considerably higher natural frequencies. Presently, there are accelerometers and hydrophones available that have unmounted fundamental natural

¹⁴Hutton, P. H., "Nuclear Reactor Background Noise U. S. Flaw Detection by Acoustic Emission," Presented at the Eighth Symposium on Nondestructive Evaluation, sponsored by American Society for Nondestructive Testing and Southwest Research Institute, San Antonio, Tex. (Apr 1971).

*In general monitoring of stress wave emissions, it is not always feasible to use longitudinal waves.

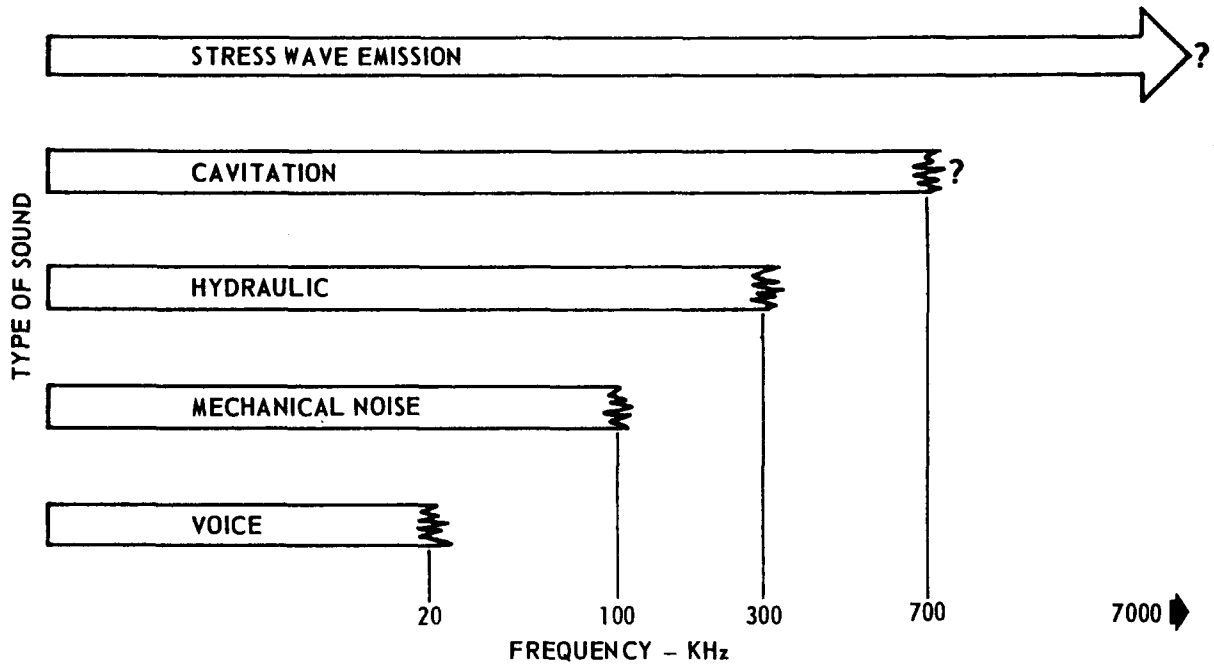


Figure 6 - Frequency Range of Various Emission Sources

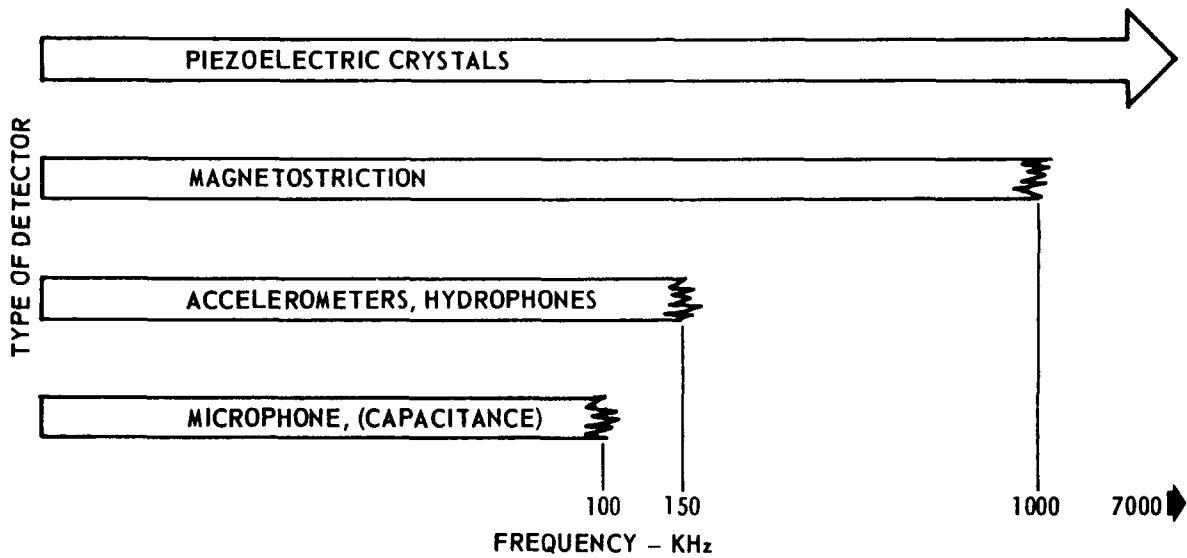


Figure 7 - Frequency Range of Various Types of Transducers

frequencies as high as 150 kHz. It is quite likely that this frequency can be increased significantly in the near future. Other sensors do exist already however that can respond with a significant output at considerably higher frequencies. For example, magnetostriction has been reported to respond to frequencies of as much as 1 MHz.¹⁵ Finally Figure 7 indicates that the response of piezoelectric crystals goes into the megahertz range.

The parameter that controls the effectiveness of the transducer is the fundamental natural frequency. This is so because so far the transducers have been excited primarily at their natural frequency by acoustic emissions, owing to the very high frequency of an acoustic emission, i.e., well into the megahertz range.

A comparison of Figures 6 and 7 indicates that using the piezoelectric crystal-type transducer would lead to optimum results. In some of the earlier work, phonograph cartridges and microphones were used; however, the general trend presently is to use piezoelectric crystals, either with (accelerometer) or without a mass. Such a choice would need to be evaluated by locating the best frequency range in which the crystal still would have acceptable sensitivity. Consequently for present work in monitoring stress wave emissions a piezoelectric crystal is recommended for use as the transducer.

SIGNAL CONDITIONER

A schematic of the signal conditioner presently in use at the Center has been shown in Figure 8. The present signal conditioner can be adjusted to all frequency ranges less than 1 MHz. The high-pass filter is a plugin card, and it is matched accurately to the transducer that is being used in order to eliminate as many of the low-frequency signals as possible. From the high-pass filter, the signal is amplified by 26 dB. An adjustable attenuator allows this amplification to be reduced to 0 dB. From the

¹⁵Lynnworth, L. C. and J. E. Bradshaw, "Magnetostriction Transducers for Acoustic Emission, Impulse, Vibration, and Noise Analysis," *Materials Research and Standards*, Vol. 11, No. 3, p. 33 (1971).

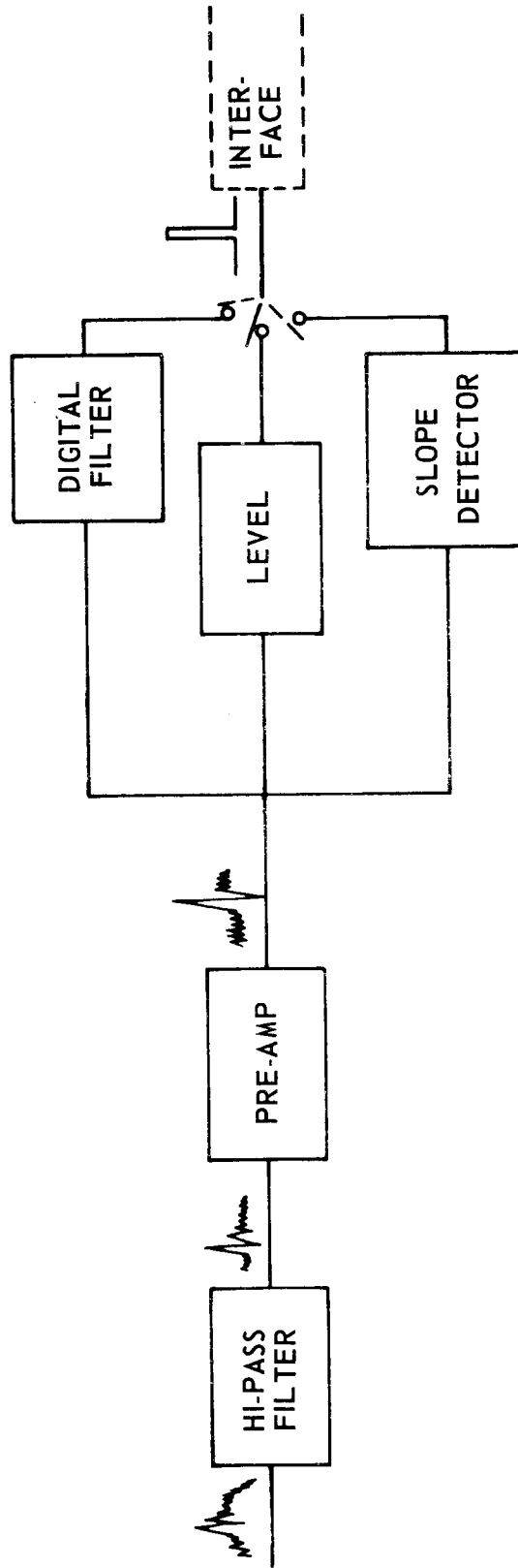


Figure 8 - Schematic of Signal Conditioner

preamplifier, the signal will be discriminated against on the basis of level, frequency or initial rise time, using the level detector, digital filter, or slope detector, respectively. A brief description of each of these components follows.

The level detector has only one function, namely, to emit one pulse for each signal that exceeds a certain preset amplitude. Figure 9a shows the principle of the level detector. In the top of the figure, the incoming wave form has been depicted. Assume, for example, that all signals larger than +E are desired, then the level detector will emit a pulse for a period during which the wave exceeds +E as shown in the center of Figure 9a. Similarly the level detector can be set to pass all signals whose amplitude is smaller than -E such as shown in the lower part of Figure 9a. The amplitude E is adjustable.

Figure 9b is a schematic of the electronics used in the level detector. The input carries the signal of interest into a comparator. The comparator examines the signal with respect to some preset value and puts out a pulse during the time that an acceptable signal is received. The level detector is useful in eliminating the electronic "grass line" or to discriminate against low-level signals.

The digital filter is a very narrow band-pass filter. In principle when a positively directed signal comes into the filter, a pulse is triggered. If these pulses come within a preset time of each other, then the pulse is let through since it has the desired period or frequency.* The triggering signals might be the pulses emitted from the level recorder.

Figure 10a shows a flow diagram of the digital filter. The level detector pulse has been shown in the top trace, i.e., a square wave. When the pulse comes in, three "one shots" are triggered. A narrow one shot N puts out a narrow pulse, i.e., $\ll 1/\text{sec}$. A long one shot L puts out a pulse equal to the period of the lowest desired frequency limit. Finally a short one shot S puts out a pulse equal to the period of the highest desired frequency limit. When all one shots are active simultaneously, then the pulse is let through.

*Higher order harmonics will also pass through the filter.

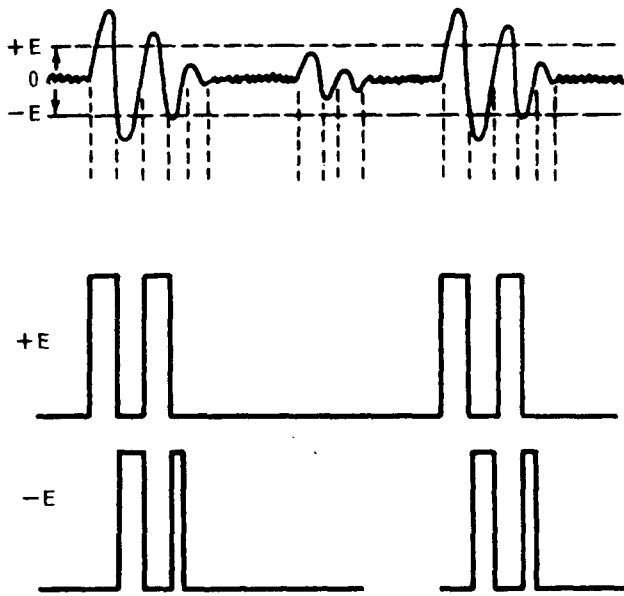


Figure 9a - Principle of Operation

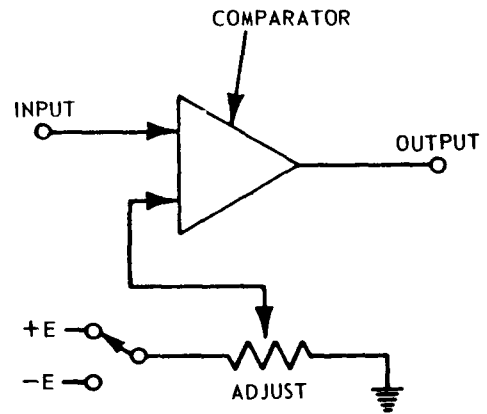


Figure 9b - Electronic Schematic

Figure 9 - Level Detector

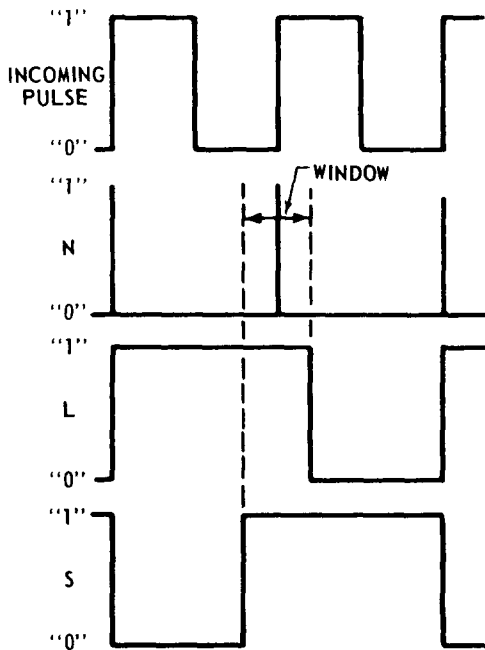


Figure 10a - Principle of Operation

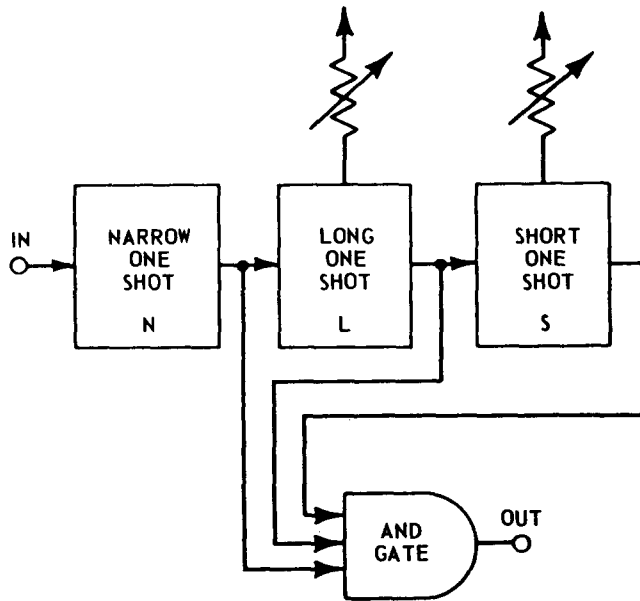


Figure 10b - Electronic Schematic

Figure 10 - Digital Filter

Figure 10b shows the schematic of the electronics used in the digital filter. As shown, the long and the short one shots are adjustable to enable adjustments of the low- and the high-frequency limits. All three one shots go into an and-gate, which will only pass a signal during the active period of all the one shots simultaneously. This kind of circuitry allows for a very narrow band-pass filter without passing a frequency that does not lie exactly within the allowed window.

The slope detector allows determination of the slope of the incoming signal, i.e., whether the initial slope is greater than some preset slope. The system determines whether the signal undergoes a set voltage differential within a known time period.

Figure 11a shows the flow diagram of the slope detector. Basically two level detectors are used. A, the first of these, triggers a one shot at a known voltage level which gives out a pulse for a selectable time duration. B, the second, triggers at a higher voltage level. If the time pulse is still active when B triggers, a pulse is passed through the output of the slope detector.

Figure 11b is the schematic of the electronics for the slope detector. An adjustable comparator A triggers the rise-time one shot T at the lower voltage level. A second adjustable comparator B emits a signal when a higher voltage level is exceeded. Both outputs from the T one shot and the B comparator are fed into an and-gate. A pulse is thus put out when both incoming signals are active.

DATA ANALYSIS

Once the acoustic emission signals have been processed through the signal conditioner, the signals are channeled through the computer interface for analysis; see Figure 5.

Figure 12 shows the interface that is utilized in the detection system for stress wave emission. The interface performs two functions. First, the interface takes signals from all the signal conditioners and passes the signals to the computer. It also lights a lamp on the channel that received the first pulse for a preset time. The computer only utilizes the first four incoming pulses. This allows enough information for the computer to do an effective analysis without cluttering the computer

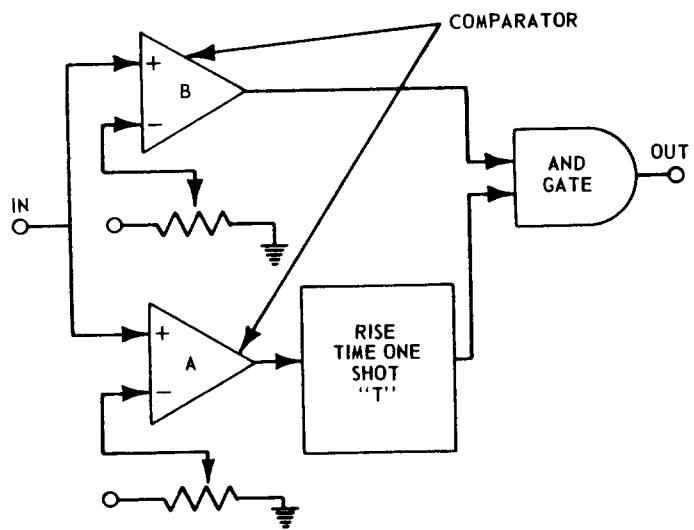
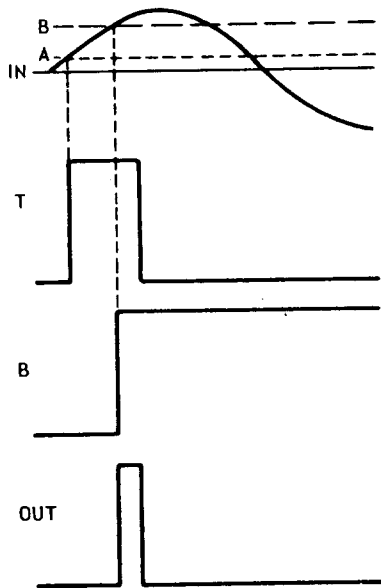


Figure 11a - Principle of Operation Figure 11b - Electronic Schematic

Figure 11 - Slope Detector

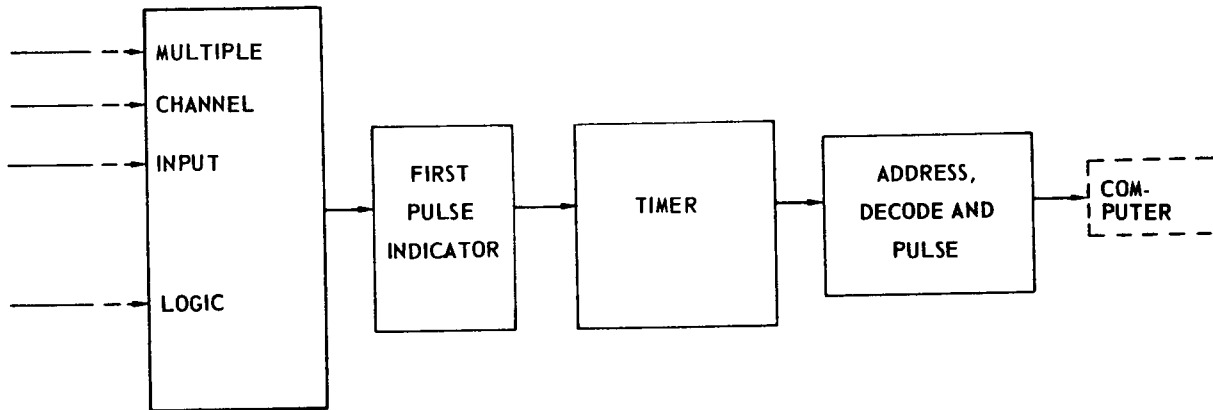


Figure 12 - Interface

components with unnecessary information. Second, the interface prepares the incoming signals for the computer by putting the signals into binary language, tagging the signals, and performing any other signal preparation prior to putting the signal into the computer. The second function is performed in the address, decode, and pulse portion of Figure 12 and will not be discussed in detail in this paper.

The multiple channel input logic, the first pulse indicator, and the timer are used to accomplish the first function of the interface; they are shown schematically in Figure 13 and are collectively called the recycle timer. All the signal conditioners are fed into a separate flip-flop unit. A typical channel has been shown in Figure 13. When a signal enters the flip-flop, it puts out two pulses as shown in Figure 13. The flip-flop will not put out more signals until it has been reset. One of these outputs is fed to the computer through a buffer gate and also to a wire or-gate. All of the channels feed into the same or-gate with a negative going pulse from the flip-flop. The other output from the flip-flop feeds into a nand-gate with a positive going pulse. Each of the N incoming channels has its own nand-gate.

The function of the or-gate is to put out a negative going pulse when a pulse comes in from any one of the N flip-flops. The or-gate will put out no other signal until it has been reset. The function of the nand-gate is to pass all pulses that are positive going. The nand-gate will be closed when a negative pulse hits it until the complete recycle timer is reset. The output from the nand-gate is fed into a one shot which will light a lamp for a preset period of time.

The negative going pulse put out by the or-gate is routed to the nand-gate so that it closes the gate. Also the or-gate pulse is fed into a delayed one shot. The amount of delay in the one shot can be adjusted. The output from the delayed one shot triggers a reset one shot, which in turn resets the complete recycle timer, thereby readying the system for the next pulse from the signal conditioner.

The recycle timer is set up so that only the light that corresponds to the channel that receives the first incoming stress wave emission will light up. In this way an approximate area is pinpointed from which the stress wave emission comes. This is accomplished as follows. The output

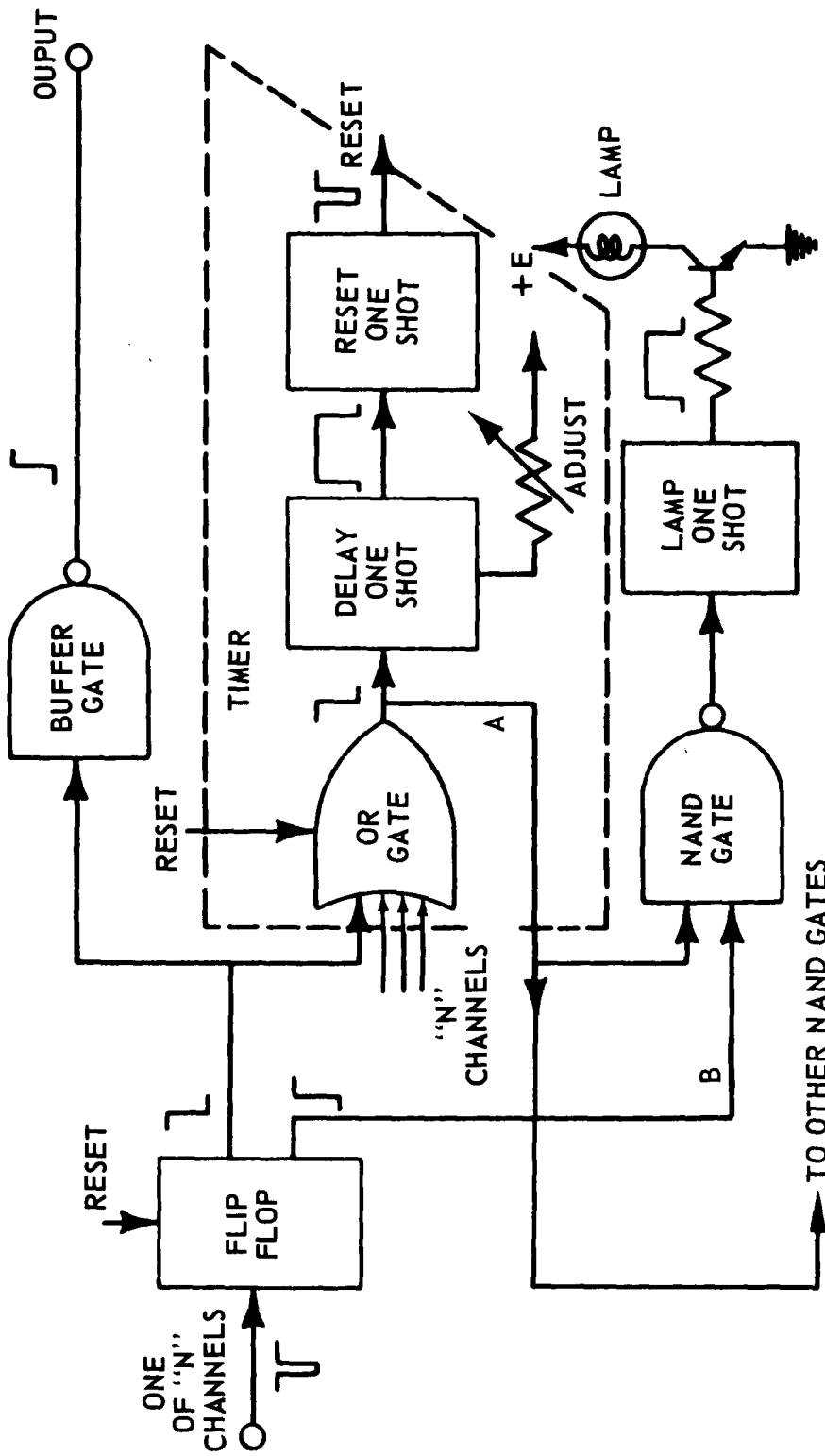


Figure 13 - Schematic of Recycle Timer

from the or-gate closes all the nand-gates. The output of the or-gate has a builtin delay of approximately 100 nsec with respect to the time of arrival to the nand-gate from the first flip flop which triggers a positively directed pulse. Thus this pulse is passed by the nand-gate. The 100 nsec is shorter however then the time difference within which the second transducer would receive the stress wave emission which has already triggered the first transducer. Consequently only one lamp will light.

As shown in Figure 5, the signals after passing through the interface are channeled to the minicomputer. The minicomputer envisioned for the system at the Center will perform various analyses of the signal and take some preprogramed action based on the analyses. The minicomputer will perform a signature analysis of the incoming signals in order to identify characteristics that can be indicative of the material and/or the structural condition of the components that are monitored. This signature analysis is based on previous characterization of the structural material; the signature analysis may also be used to do a material characterization.

The minicomputer will also provide the computations needed for triangulation of flaws or other emission sources that require attention. As has been stated the computer only utilizes the first four incoming pulses, allowing an effective analysis without cluttering the computer components with unnecessary information. Based on the results of the triangulation, cross correlation will be used to achieve spatial discrimination of the emissions. Finally when using monitoring techniques for stress wave emissions on standard tests such as, for example, in fracture or fatigue tests, creep tests, tensile tests, and others, the minicomputer can analyze test results in real time so that considerable control can be held on the testing program. Additionally the use of data from stress wave emissions can increase the amount of data that may be collected from standard tests.

The minicomputer can also initiate an action. Primary among the action is the ability of the minicomputer to assume control in a critical application when time is of the essence. For example, in hydrostatic testing of pressure hulls, the minicomputer might automatically initiate unloading of the hull when a catastrophic failure is about to ensue.

Human reaction time could be too slow in such cases. Potentially such a system might be installed on nuclear reactor pressure vessels or submersibles.

Sources of stress wave emissions can be displayed through the minicomputer on consoles or television monitors. Through the use of such display and in conjunction with characterization analysis, the minicomputer may request that other kinds of nondestructive testing procedures be utilized in order to determine the severity of an emission source. This is particularly important since an already existing flaw will only produce emission when the flaw continues to grow and stress wave emissions give no indications about the extent of the existing flaw.

The minicomputer can also act as an agent to alter operational requirements of certain structures. For example, in nuclear reactor pressure vessels, the minicomputer might call for a decrease in the maximum allowable operating pressure. This same philosophy can of course be extended to other structures as well.

Finally the minicomputer may disregard certain emissions when it decides that they are extraneous signals, e.g., using spatial discrimination techniques. Additionally the minicomputer can record or store all the events that it has accepted as being true stress wave emissions.

SYSTEM CONSTRUCTION

Figure 14 shows the present stress wave-monitoring capability at the Center. Construction of the system was initiated by breadboarding a 1-channel signal conditioner. This unit was checked out and debugged. Subsequently 10 channels of signal conditioning units modeled after the breadboard were constructed. The 10 channel unit can be seen in Figure 14. The present signal conditioners can be adjusted to all frequency ranges less than 1 MHz. The high-pass filter is a plugin card and is matched accurately to the transducer that is being used in order to eliminate as many of the low-frequency signals as possible. From the high-pass filter, the signal is amplified by 26 dB. An adjustable attenuator allows this amplification to be reduced to 0 dB.

The raw or conditioned signals can be recorded on tape for future analysis. The reel-to-reel tape recorder currently in use is a Honeywell

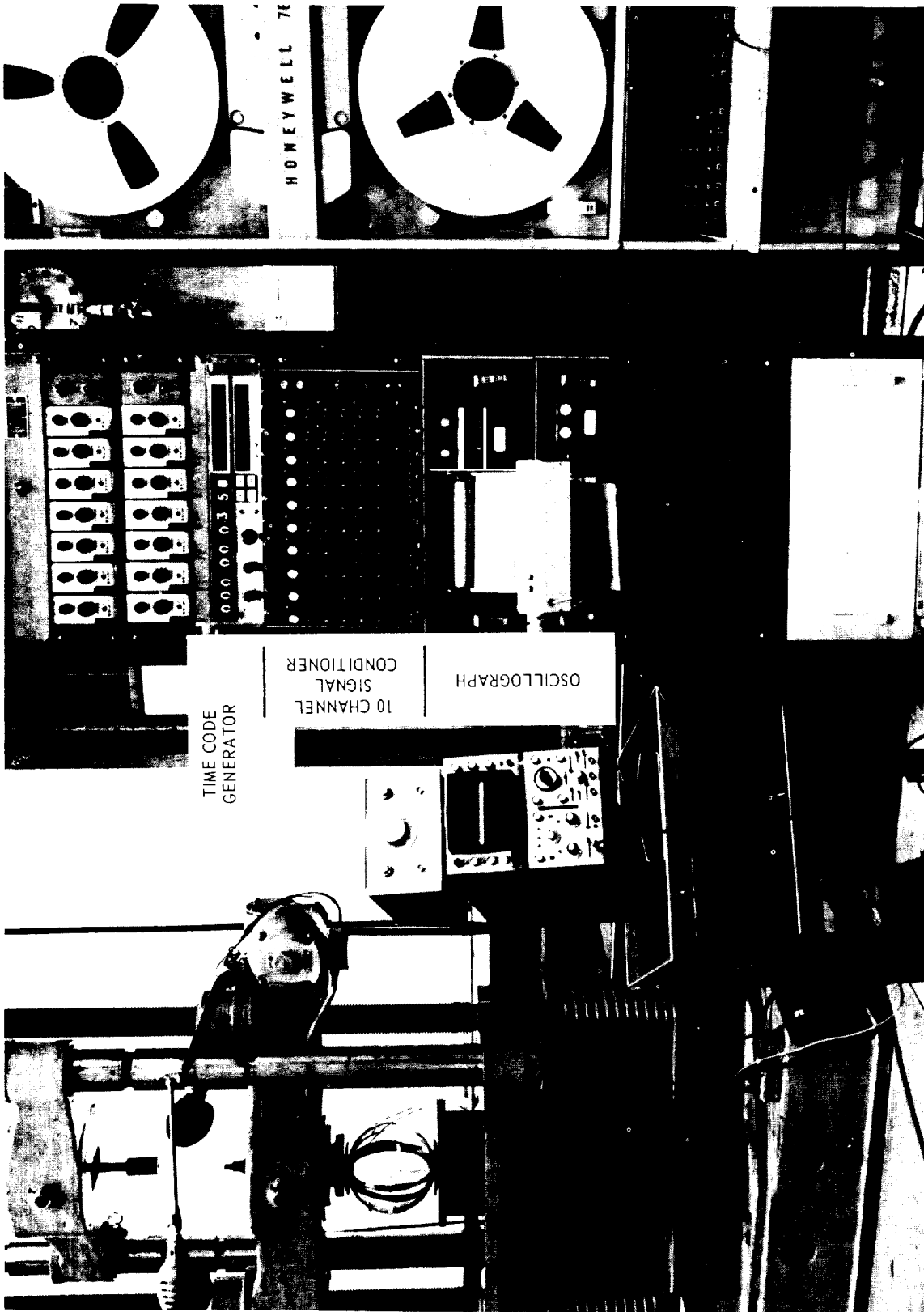


Figure 14 - System for Monitoring Stress Wave Emissions

Model 7600 and can be seen in Figure 14. The recorder has 14 channels of direct record-and-reproduce electronics and two edge tracks. One of the edge tracks is used for voice comment, the other may be used as desired. Except for the bandwidth, the Model 7600 record is built to IRIG (inter range instrumentation group) specifications. The dynamic characteristics of the direct record-and-reproduce electronics are listed.

Tape Speed ips	Bandwidth Hz ± 3 dB	RMS Signal/RMS Noise dB Unfiltered
120	400 - 700,000	28
60	400 - 250,000	28
30	400 - 125,000	28
15	300 - 125,000	28
7 1/2	200 - 62,500	26
3 3/4	200 - 31,250	24

The tape recorder is equipped with a time-code generator-translator and tape-search unit, Systron Donner Model 8154, which stores time on one channel of magnetic tape for retrieval.

Once data are stored on tape, the data can be analyzed in greater detail through permanent oscillographic records. The oscillograph in use is a Bell and Howell Datagraph S-134 with a maximum speed of 100 ips. Thus, if a tape recording is made at 120 ips, played back at 1 7/8 ips, and reproduced on the oscillograph at 100 ips, a time-base expansion of 6400 is attained.

SYSTEM APPLICATION

The acoustic emission system described in the previous section has been applied in a recent test at the Center. Two glass hemispheres were taped together and were loaded by compression at the apex of the hemispheres. Three different series of crystals were cemented to each hemisphere at equal distances from the apex. Figure 15 shows the two hemispheres. The crystals are PZT piezoelectric crystals and have the dimensions shown in Figure 16. This figure also shows the location of the crystals on the hemisphere.



Figure 15 - Two Glass Hemispheres Subjected to Compressive Loadings

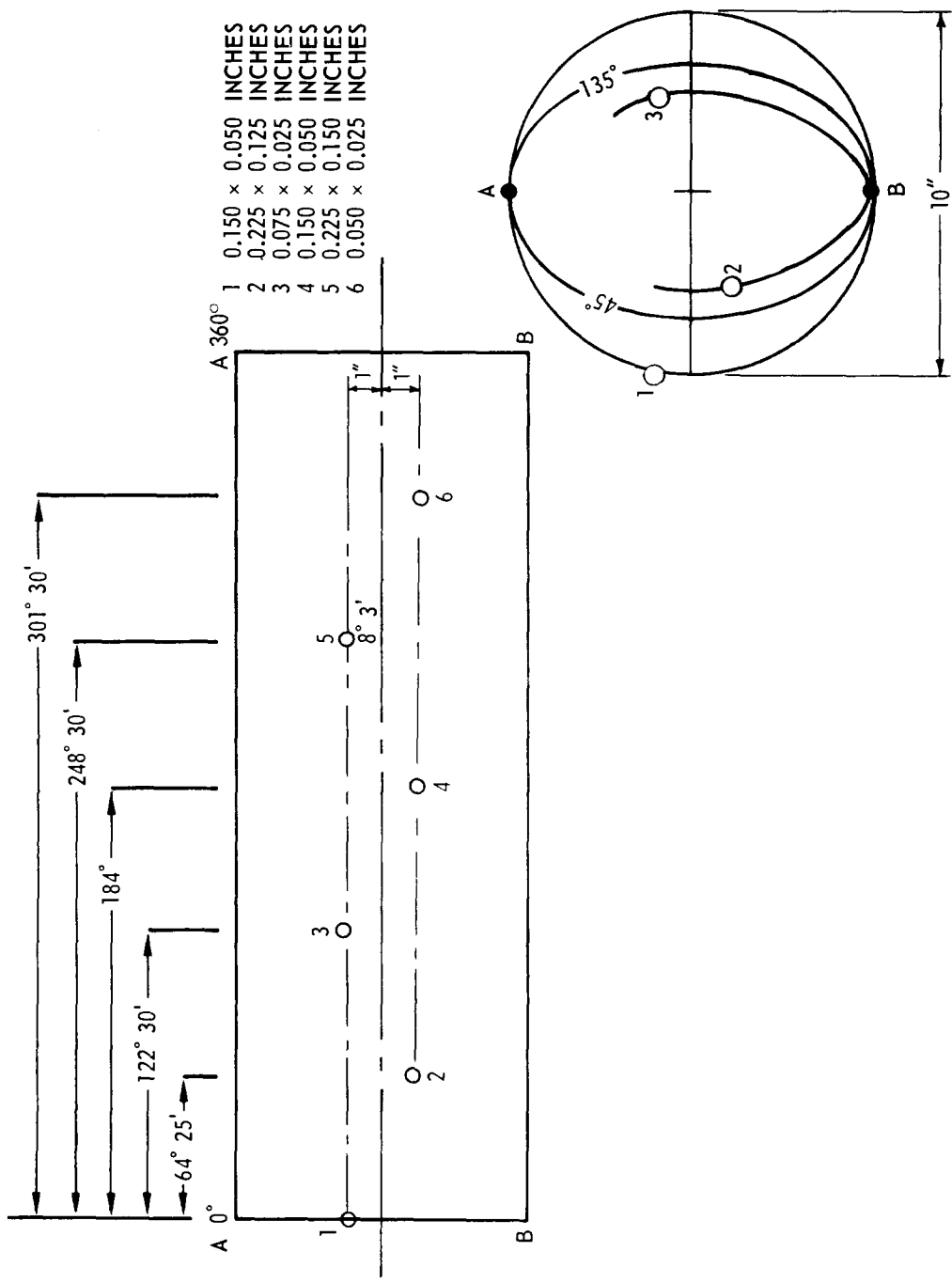
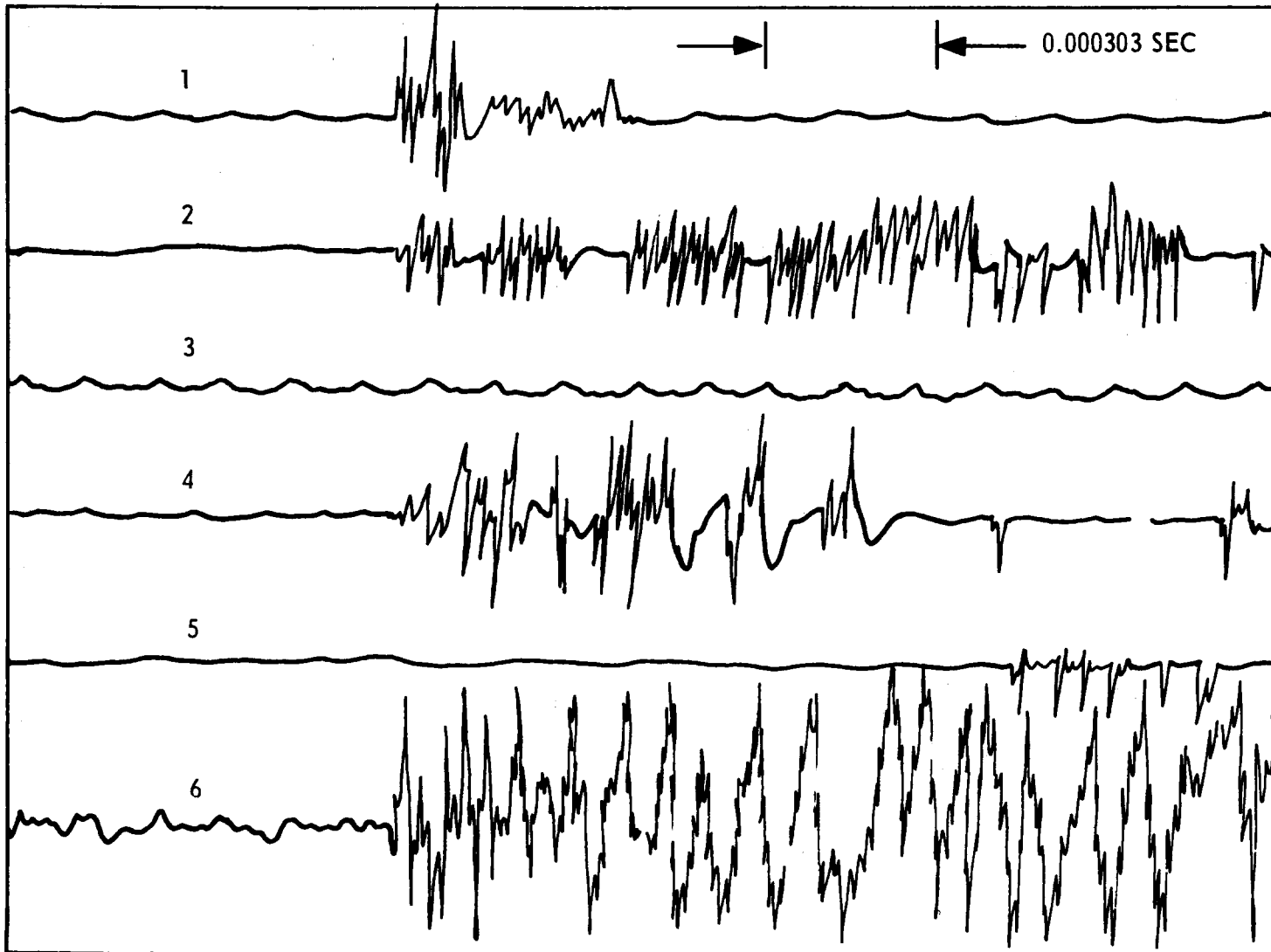


Figure 16 - Transducer Layout on Glass Hemispheres



10303 SEC

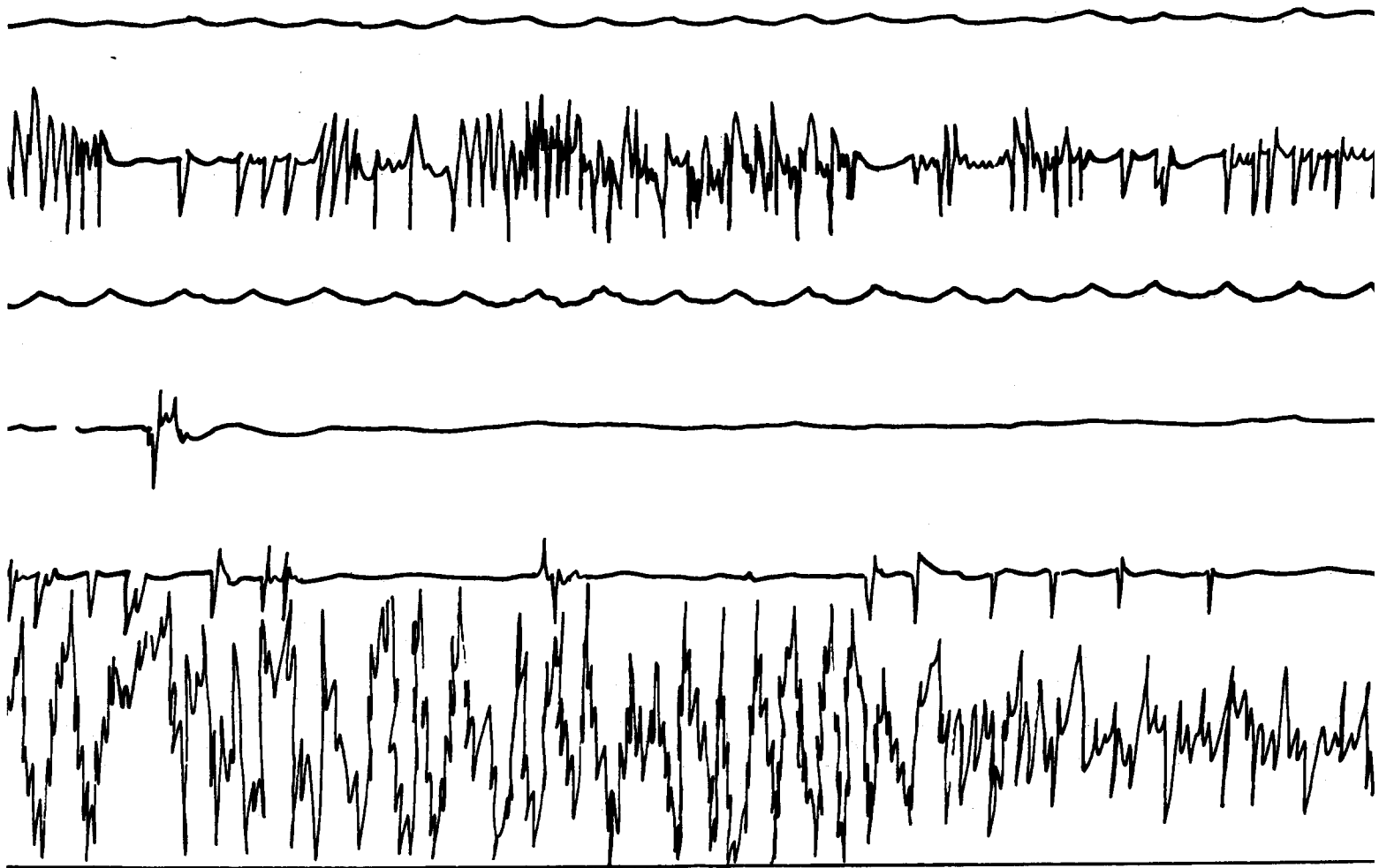
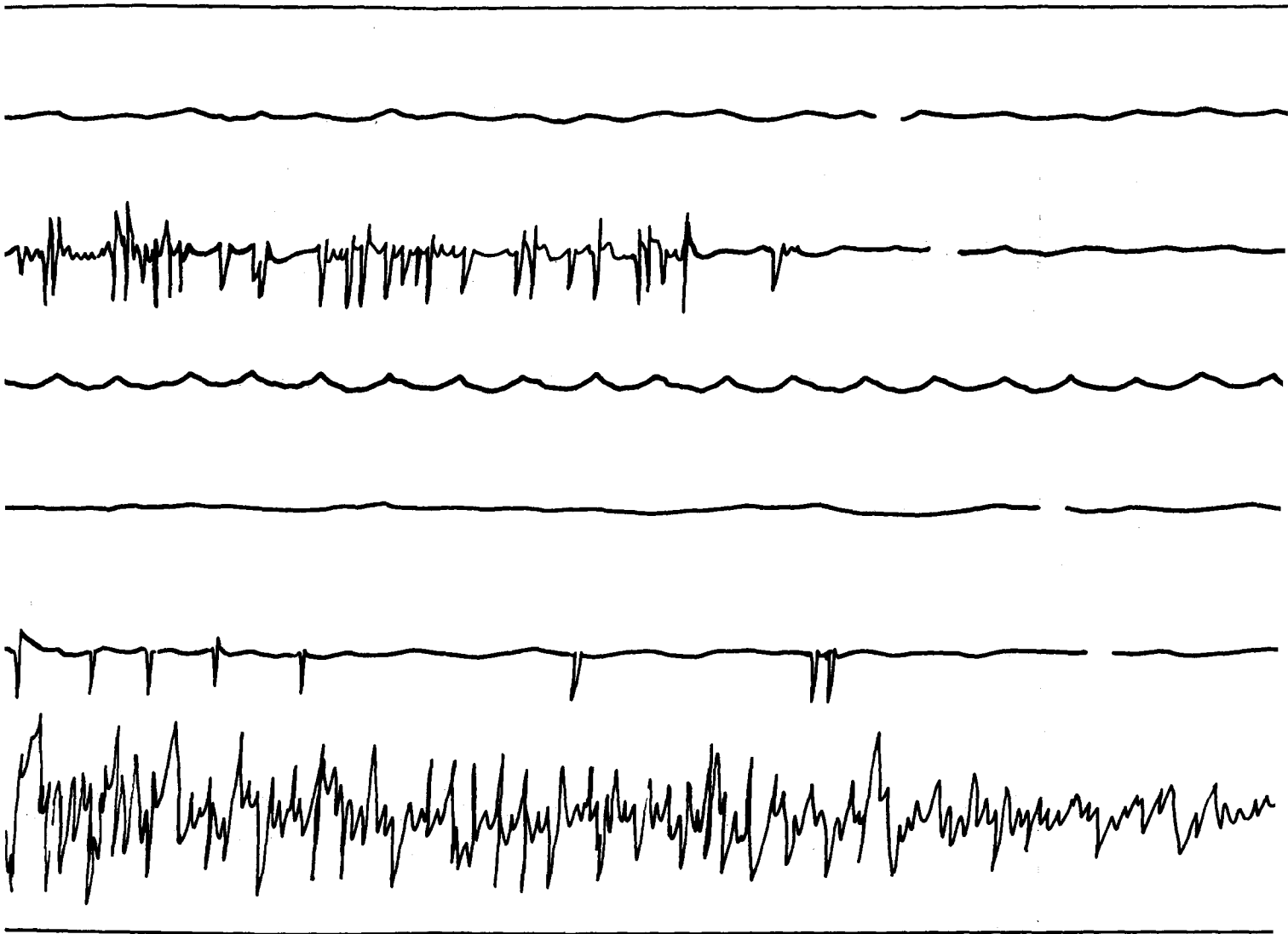
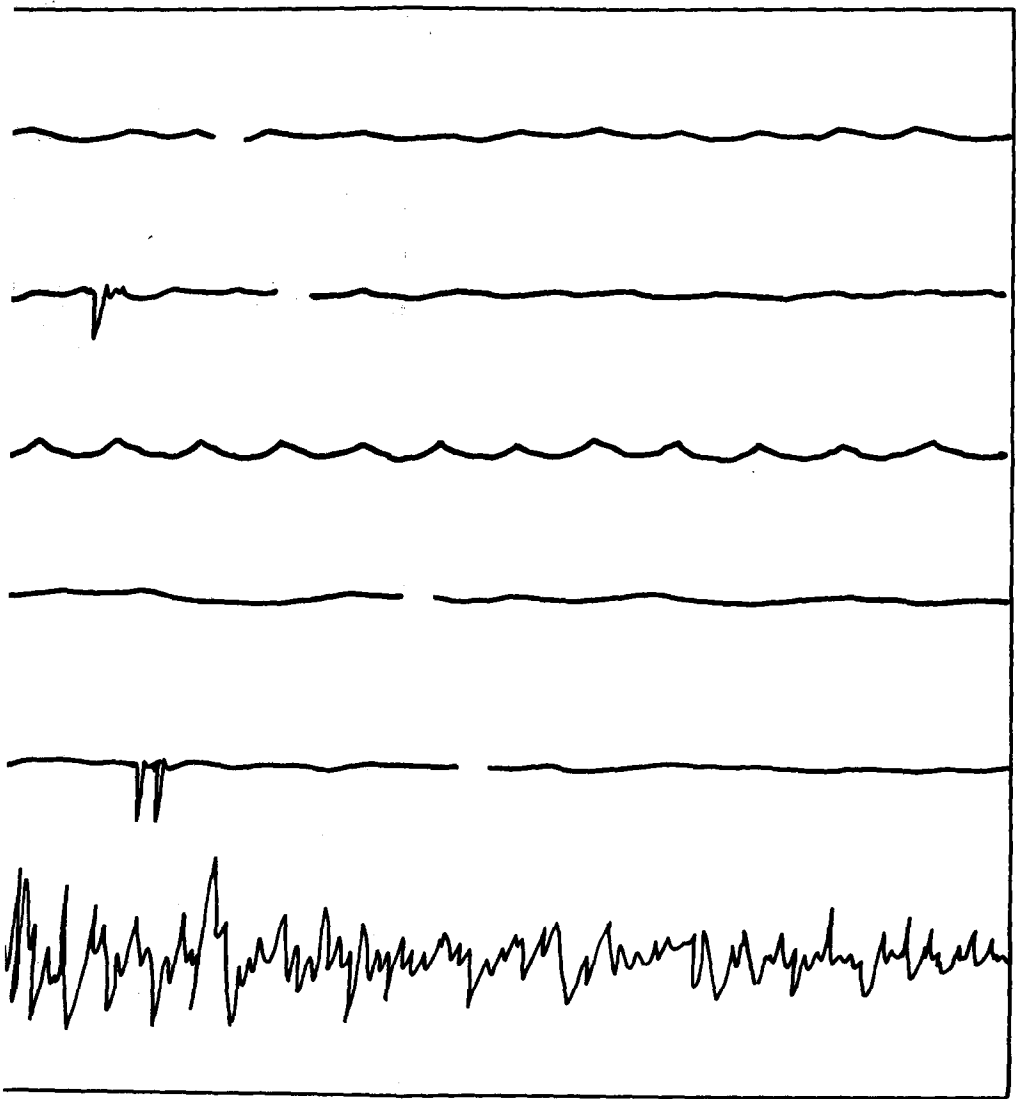


Figure 17 - Level Recording from Glass Hemispheres



Hemispheres



data analysis. As has been discussed, each material exhibits acoustic emissions that are characteristic to that material. Therefore, a smaller system (4 channels) is presently under construction which has as its primary function the characterization of materials.

Generally there are various stages at which monitoring of stress wave emissions is an important link. It is useful in fabrication monitoring, e.g., welds, and in laboratory testing, e.g., pressure hull models.

In the fabrication aspect, particular attention will be given to delayed weld cracking. In addition, however, other aspects of the manufacturing process will be considered. As an example, the integrity of liners in pressure tanks can be evaluated. Not to be overlooked is the already shown monitoring of stress wave emissions in proof-testing pressure vessels at either completion of fabrication or various intervals during the life of the vessel.

In laboratory applications, monitoring of stress wave emissions will be specifically oriented to overcoming the interference effects caused by hydraulic noise. To this end the use of single crystals has been initiated (as in the glass sphere discussed previously). This should enable using much higher cutoff frequencies without losing the acoustic emission signal. Other procedures will also be considered, however, if they appear more useful. It is believed at this point that the problem of hydraulic noise is the largest obstacle to completion of the monitoring system for stress wave emissions; consequently, a significant effort will be directed to solution of the hydraulic noise problem.

A continual reappraisal of the overall program will be conducted, based on the results obtained from application of the monitoring system for stress wave emissions. This will ensure that the final system will incorporate the latest thinking in monitoring of stress wave emissions.

SUMMARY

The foregoing discussion has been concerned with a state-of-the-art survey of the phenomena of stress wave emissions. Specific instrumentation requirements are discussed. Several monitoring applications from the literature as well as applications at the Center have been discussed. Finally the current program for developing a monitoring system at the Center has been detailed.

ACKNOWLEDGMENTS

Monitoring of stress wave emissions at the Center was first made possible by interest and support from Mr. H. Bernstein. Currently the interest and support from Mr. B. B. Rosenbaum is appreciated. The encouragement received from Messrs. M. A. Krenzke and T. J. Kiernan is acknowledged. The design and construction of the electronics used in the present Center system was done by Mr. D. T. Milne. Finally many valuable suggestions made by Mr. K. Nishida are appreciated.

REFERENCES

1. Kaiser, J., "Untersuchungen uber das auftreten Gerauschen beim Zugversuch," Ph.D. thesis, Technische Hochschule, Munich (1950).
2. Jolly, W. D., "Acoustic Emission Exposes Cracks during Welding," *Welding Journal* Vol. 48, No. 1, pp. 21-27 (Jan 1969).
3. Hartbower, C. E., "Application of Stress Wave Analysis Technique to the Nondestructive Inspection of Welds," *Welding Journal*, Vol. 49, No. 2, p. 54S (Feb 1970).
4. Dunegan, H. L. et al., "Detection of Fatigue Crack Growth by Acoustic Emission Techniques," *Materials Evaluation Journal*, Vol. 28, No. 10, pp. 221-227 (Oct 1970).
5. Paris, P. C., "The Fracture Mechanics Approach to Fatigue," *Proceedings 10th Sagamore Conference*, Syracuse University Press, N. Y., p. 107 (1965).
6. Lomacky, O. and H. Vanderveldt, "Critical Review of Fracture and Fatigue Analysis," *NSRDC Report 3655* (1971).
7. Gerberich, W. W. and C. E. Hartbower, "Monitoring Crack Growth of Hydrogen Embrittlement and Stress Corrosion Cracking by Acoustic Emission," *Proceedings of Conference on Fundamental Aspects of Stress Corrosion Cracking*, Ohio State University, National Association of Corrosion Engineers, pp. 420-438 (1967).

8. Coe, F. R. and J. Morebon, "Estimation of Diffusibility Coefficients for Hydrogen in Ferrous Materials," British Welding Journal, Vol. 43 (1967).

9. Ord, R. N., "Acoustic Emission Detection of Dislocation Movement and Crack Growth in HY-80 Ferritic Steel," Batelle Memorial Institute (NW) Report Y 49034 to the Naval Ship Research and Development Center (1969).

10. Frederick, J. R., "Dislocation Mechanisms as Sources of Acoustic Emission," Presented at the Symposium on Advanced Nondestructive Testing Techniques, sponsored by Advanced Research Projects Agency and Army Materials Mechanics Research Center, Watertown, Mass. (Jun 1971).

11. Chambers, R. H., "Time and Frequency Domain Analysis of Acoustic Emission during Fatigue Failure," Presented at the Symposium on Advanced Nondestructive Testing Techniques, sponsored by Advanced Research Projects Agency and Army Materials and Mechanics Research Center, Watertown, Mass. (Jun 1971).

12. Gerberich W. W. and W. G. Reuter, "Theoretical Model of Ductile Fracture Instability Based on Stress-Wave Emission," Final Report to Office of Naval Research, Aerojet General Corporation Contract N00014-66-C-0340 (Feb 1969).

13. Gilman, J. S., Proceedings of the Fifth U. S. National Congress on Applied Mechanics, American Society of Testing Materials, New York, p. 385 (1966).

14. Hutton, P. H., "Nuclear Reactor Background Noise U. S. Flaw Detection by Acoustic Emission," Presented at the Eighth Symposium on Nondestructive Evaluation, sponsored by American Society for Nondestructive Testing and Southwest Research Institute, San Antonio, Tex. (Apr 1971).

15. Lynnworth, L. C. and J. E. Bradshaw, "Magnetostriction Transducers for Acoustic Emission, Impulse, Vibration, and Noise Analysis," Materials Research and Standards, Vol. 11, No. 3, p. 33 (1971).

INITIAL DISTRIBUTION

Copies

1 DIR DEF, R&E
 1 CNO
 1 Tech Analy & Adv Gr
 (OP 07T)
 1 CHONR
 Attn: Struc Mech Br
 (Code 439)
 5 NRL
 2 Code 6381
 3 Code 8430
 1 NAVMAT (MAT 0331)
 17 NAVSHIPSYSCOM
 1 PMS 381
 1 PMS 391A.5
 1 PMS 393
 1 PMS 394
 1 PMS 395AZ
 1 PMS 396
 1 PMS 397
 1 PMS 399
 1 SHIPS 034
 1 SHIPS 0342
 1 SHIPS 03421
 1 SHIPS 03422
 1 SHIPS 03423
 1 SHIPS 03424
 2 SHIPS 2052
 1 SHIPS 425TH
 2 NAVFAC ENG CMD
 1 CHES NAVFAC
 Mr. F. Gorman
 1 2C45A
 Mr. A. Ianuzzi
 2 NADC (ST-3)
 1 CDR, NELC
 2 NURDC
 1 Code 6505
 1 Code 6523
 1 NAVCOASYSLAB
 Attn: Mr. Mossbacher
 2 NOL
 1 Code 211
 1 Code 2302

Copies

1 NWL, Dahlgren, Va.
 1 NUSC, NEWPT
 1 NUSC, NLOND
 1 SUPT, USNA
 1 SUPT, PGSCHOL, Monterey
 1 CO, USNROTC & NAVADMINU, MIT
 1 Naval War College
 12 NAVSEC
 1 SEC 6101
 4 SEC 6101D
 1 SEC 6105
 1 SEC 6113
 1 SEC 6128
 3 SEC 6129
 1 SEC 6140
 1 NAVSHIPYD CHASN
 1 NAVSHIPYD PTSMH
 1 NAVSHIPYD SFRANBAY VJO
 1 SUPSHIP, Groton
 12 DDC
 1 NASA Lewis Research Center
 Attn: Prof. J. E. Srawley,
 1 U. S. Geological Survey
 345 Middlefield Road
 Menlo Park, Calif. 94025
 Attn: Dr. J. D. Byerlee
 1 Brown University
 Dept of Applied Mathematics
 Providence, Rhode Island 02912
 Attn: Prof. H. Kolsky
 1 George Washington Univ
 School of Engineering and
 and Applied Science
 Washington, D. C.
 Attn: Dr. H. Liebowitz
 1 Lehigh Univ
 Mechanics Department
 Bethlehem, Pa.
 Attn: Prof. G. Sih

Copies

1 Pennsylvania State Univ
Dept of Mining
118 Mineral Industries Bldg
University Park, Pa. 16802
Attn: Dr. H. R. Hardy

3 Southwest Research Institute
1 Prof. R. DeHart
1 Mr. D. Rinehart
1 Dr. S. P. Ying

1 Univ of Calif, Berkeley
Lawrence Radiation Lab
Attn: Prof. C. Tatro

2 Univ of Calif, Los Angeles
School of Engineering and
Applied Science
Materials Dept
Los Angeles, Calif.
1 Dr. A. S. Tetelmen
1 Dr. K. Ono

1 Univ of Michigan
Dept of Mech Engineering
Ann Arbor, Michigan
Attn: Prof J. R. Frederick

2 Aerojet General Corp
Metallurgy Section
Advanced Technology
Sacramento, Calif. 95813
1 Mr. C. Hartbower
1 Mr. C. Morais

3 Battelle Northwest Lab
Richland, Wash. 99352
1 Mr. J. Vetrano
1 Mr. D. Jolly
1 Mr. P. Hutton

1 Boeing Company
Aerospace Group
P. O. Box 3999
Seattle, Wash. 98124
Attn: Mr. F. J. Duvall

1 Del Research Corporation
427 Main Street
Hellertown, Pa. 18055
Attn: Prof. P. Paris

Copies

3 Dunegan Research Corp
2044 Research Drive
Livermore, Calif. 94550
1 Mr. H. Dunegan
1 Dr. D. Harris
1 Mr. A. Green

1 Esso Research and Engineering
Company
Florham Park, N. J. 07932
Attn: Mr. N. O. Cross

1 Excelco Develop, Inc
Silver Creek, N. Y.
Attn: Mr. W. D. Abott

2 General Dynamics Corp
1 Convair Aerospace Div
Fort Worth, Texas
Attn: Dr. Y. Nakamura
1 Electric Boat Div
Groton, Conn.
Attn: Mr. J. M. Cameron

1 Lockheed Missiles and
Spacecraft Company
Sunnyvale, Calif.
Attn: Mr. G. Nichol

1 North American Rockwell
Space Division
12214 Lakewood Blvd
Downey, Calif. 90241
Attn: Mr. J. Rynewicz

1 Timet Corp
West Caldwell, N. J.
Attn: Mr. N. Fiege

1 U. S. Steel Corp
Edgar C. Bain Laboratory
Research Center
Monroeville, Pa. 15146
Attn: Mr. G. R. Speich

1 Westinghouse Corporation
Pittsburgh, Pa.
Attn: Dr. S. K. Chan

CENTER DISTRIBUTION

Copies	Code	
1	172	M. Krenzke
1	1721	
1	1725	
10	1727	T. Kiernan, K. Nishida
1	173	
1	174	
1	177	
1	178	
1	27	
1	28	
1	282	
1	2821	
1	2822	
5	2823	
	5	H. Vanderveldt
1	29	
2	296	

DOCUMENT CONTROL DATA - R & D

(Security classification of title, body of abstract and indexing annotation must be entered when the overall report is classified)

1. ORIGINATING ACTIVITY (Corporate author) Naval Ship Research and Development Center Bethesda, Maryland 20034		2a. REPORT SECURITY CLASSIFICATION UNCLASSIFIED	
2b. GROUP			
3. REPORT TITLE MONITORING STRESS WAVE EMISSIONS			
4. DESCRIPTIVE NOTES (Type of report and inclusive dates)			
5. AUTHOR(S) (First name, middle initial, last name) Hendrikus H. Vanderveldt			
6. REPORT DATE June 1972		7a. TOTAL NO. OF PAGES 42	7b. NO. OF REFS 15
8a. CONTRACT OR GRANT NO.		9a. ORIGINATOR'S REPORT NUMBER(S) 3809	
b. PROJECT NO. Task Area S4616, Task 11896		9b. OTHER REPORT NO(S) (Any other numbers that may be assigned this report)	
c. Task Area S-F51.541.009, Task 15916			
d.			
10. DISTRIBUTION STATEMENT APPROVED FOR PUBLIC RELEASE: DISTRIBUTION UNLIMITED			
11. SUPPLEMENTARY NOTES		12. SPONSORING MILITARY ACTIVITY NAVSHIPS PMS 395 (Formerly DSSPO) NAVSHIPS 034	
13. ABSTRACT <p>Basic principles of the acoustic-emission technique used at the Center are discussed, and a review of some applications of the method are presented. Potential capabilities and drawbacks to naval applications are summarized; finally, a description of the design and construction of the present monitoring capability at the Naval Ship Research and Development Center is presented.</p>			

UNCLASSIFIED

Security Classification

14. KEY WORDS	LINK A		LINK B		LINK C	
	ROLE	WT	ROLE	WT	ROLE	WT
Acoustic Emissions						
Stress Waves						
Nondestructive Testing						
Fatigue						
Fracture						